Solubilities in Liquid Zinc

Zirconium, Niobium, Molybdenum, Palladium, and Thorium

ALLAN E. MARTIN, JAMES B. KNIGHTON, and HAROLD M. FEDER
Chemical Engineering Division, Argonne National Laboratory, Argonne, Ill.

STUDIES of the chemistry of liquid metal solutions were initiated because of possible applications to the refinement of nuclear materials (*3*). This article reports the solubilities of zirconium, niobium, molybdenum, palladium, and thorium in liquid zinc, as well as other information concerning zinc-rich regions of the phase diagrams.

The methods available for determination of the liquidus lines in a solvent-rich metallic system include chemical analysis of samples of the saturated liquids, thermal analysis, microscopic examination, and electrical conductivity measurements. The sampling method has certain advantages; the approach to equilibrium from either direction can be experimentally observed, low solubilities can be measured, and the over-all composition of the alloys need not be known.

Various techniques for withdrawal of samples of saturated liquids in metal systems have been described. Transfer of portions of the settled liquid by suction into a pipet has been frequently used, but can give misleading results, particularly at low concentrations of solute, because of accidental inclusion of fine particles of the solid phase in the sample. To reduce errors from this source in this study, special precautions, described in the procedure, were adopted.

EXPERIMENTAL

Materials

Zinc	Bars 99.99% Zn, 0.0015% Pb, 0.0020% Cu
Zirconium	Crystal bars, 12-mm. diameter (surfaces ground to remove oxide), 99.9% Zr
Niobium	Rods, 6-mm. diameter (spectrochemical analysis showed no more than 0.1% of any metallic impurity), sheet 0.8 mm. thick, powder 99.5% Nb
Molybdenum	Rods and sheet 99.95% Mo, 0.01% Ni, 0.01% Si
Palladium	Powder 99.5% Pd
Thorium	Rods, 9 mm., 99.9% Th, 0.1% Na, 0.05% Ca, 0.05% Be, 0.05% K

Helium was purified by passage through charcoal traps cooled with liquid nitrogen.

Apparatus. The gas-tight solubility apparatus shown in Figure 1 was designed to facilitate repeated sampling of the melt without air contamination.

The inner surface of each sampling pipet, *Q*, was precoated with a thin layer of magnesia or boron nitride, applied as a slurry and flame-dried. These coatings reduced the incidence of pipet breakage within the furnace chamber after sampling and prevented adherence of the glass to the cooled samples. A porous graphite filter, *R*, effective for removal of particles larger than 12 microns, was press-fitted into the open end of each pipet. Each filter was inspected for fit with a low-power magnifying lens.

Melt temperatures in the solubility studies were measured to an accuracy of ± 0.5° C. with calibrated Chromel-Alumel thermocouples. (Temperatures in the thermal analysis studies were measured to an accuracy of ± 0.2° C. with calibrated Pt/Pt–10% Rh thermocouples.)

Procedure. With a degassed crucible containing about 0.5 kg. of charge in place, the furnace chamber was evacuated and flushed several times with purified helium. The final pressure was maintained at about 100 mm. above atmospheric pressure. The temperature was raised to a desired "holding temperature" and maintained for at least 2 hours while the melt was stirred. Stirring was stopped and at least 15 minutes was allowed for settling. The tip of the sampling pipet was lowered to the hot zone, held there for several minutes, and then immersed in the melt. The gas pressure in the furnace was increased by about 300 mm. to force liquid through the filter and into the pipet to a height of about 10 cm. (Suction on an open-end pipet was a less reliable means for removing samples of predetermined size.) The pipet was raised to a colder region of the furnace. During the cooling, drainage of any liquid sample from the pipet was prevented by the filter. The pipet was withdrawn and the sample freed by breakage and removal of the glass.

Stirring was resumed, the temperature raised or lowered to the next holding temperature, and the procedure repeated. When the holding temperature was approached from a higher temperature, the melt was cooled slowly to favor growth of existing crystals rather than production of new crystals.

Analysis. To avoid errors due to segregation during cooling, an entire sample of about 4 grams was dissolved, and aliquots were used for duplicate analyses. The solute elements were determined spectrophotometrically.

RESULTS AND DISCUSSION

Table I contains the selected solubility data. When more than one sample was taken at a holding temperature in a series of experiments, the mean value was usually selected; however, if the values showed a trend consistent with the direction of approach to equilibrium, only the final value was selected. A further criterion in the selection of data was the consistency of values obtained with rising and falling temperatures or from different experimental series.

In Figures 1 to 4 the solubility data are shown in plots of the logarithm of the solubility *vs.* the reciprocal of the absolute temperature. An abrupt change of slope of a liquidus line is evidence of peritectic—i.e., incongruent—melting. Each new peritectic thus indicated was confirmed by thermal analysis, metallographic examination, or x-ray identification of the phases.

The solubility data for the five elements were fitted by the least-squares method to empirical equations of the form

$$\log X = A - B \times 10^3 T^{-1} + C \times 10^6 T^{-2}$$

where X is the atom fraction of solute. These equations and the values of s_{obsd}, the standard deviation in per cent of X, are given in Table II. The quadratic equation rather than the best linear equation was adopted only when the statistical F-test indicated that the fit was significantly better—i.e., by a greater than three to one chance (*14*).

Zirconium. The liquidus lines obtained in this work and by Gebhardt (*5*) and Chiotti and Kilp (*2*) are shown in Figure 2. The intersection of the two segments of the solubility line at about 548° C. evidently corresponds to the temperature of the peritectic decomposition of $ZrZn_{14}$ to form $ZrZn_8$ and melt, established (*2, 5*) by thermal analysis (at 545° C.).

The composition of the eutectic on the zinc-rich side of the phase diagram was estimated from our solubility data as 0.02 weight %. The eutectic temperature calculated from this composition and the heat of fusion of zinc is about 0.07° below the melting point of zinc, 419.5° C. The previously reported eutectic temperatures were significantly lower— 416° (*5*) and 417° ± 1° C. (*2*). Consequently, we also measured the eutectic temperature by thermal analysis;

Table I. Solubilities in Liquid Zinc

Temp., ° C.	Wt. % Solute	Temp., ° C.	Wt. % Solute	Temp., ° C.	Wt. % Solute
Zirconium[a]		Niobium[b]		Palladium[c]	
762.0	8.10	750.7	0.222	749.7	11.6
729.3	6.16	702.8	0.163	718.0	9.47
727.5	6.67	651.3	0.120	699.0	8.34
711.3	5.23	601.1	0.103	674.0	6.78
676.5	3.77	600.9	0.0931	654.8	5.53
672.5	3.84	560.6	0.0841	604.2	3.39
654.5	3.04	547.3	0.0759	550.0	2.07
624.7	2.42	518.8	0.0727	525.3	1.67
598.0	1.71	499.8	0.0728	510.0	1.35
570.2	1.35	478.9	0.0702	503.2	1.24
554.5	1.14	474.4	0.0698	482.5	0.919
524.5	0.505	462.8	0.0520	457.9	0.712
499.8	0.242	449.6	0.0420	456.2	0.686
477.5	0.124	442.4	0.0348	438.8	0.571
447.3	0.0479	439.4	0.0367		
430.9	0.0285	433.9	0.0290		
426.1	0.0277	427.9	0.0240		
Thorium[d]		Molybdenum[e]			
746.2	1.23	730.5	0.0213		
703.8	0.639	726.9	0.0224		
694.9	0.541	690.3	0.0224		
644.7	0.247	664.3	0.0216		
609.8	0.123	652.5	0.0224		
601.1	0.111	635.3	0.0227		
548.4	0.0373	593.3	0.0213		
526.6	0.0231	550.4	0.0225		
496.2	0.0113	527.1	0.0145		
475.5	0.00708	502.4	0.0122		
455.0	0.00465	450.7	0.00636		
448.9	0.00426	422.4	0.00314		

[a] Alumina crucible, Ta stirrer rod. [b] Alumina crucible, Ta or Nb stirrer rod (Nb rod also source of solute). [c] Alumina or graphite crucible, Ta stirrer rod. [d] Alumina or graphite crucible, W or Ta stirrer rod. [e] Alumina crucible, Mo stirrer rod (Mo rod also source of solute).

Table II. Constants for Solubility Equations[a]

Solute	Temp. Range, ° C.	A	B	C	s_{obsd}	Equation
Zr	425–545	19.220	25.995	6.958	5.7	1
	545–750	5.582	9.692	2.768	4.3	2
Nb	428–478	3.029	4.749	...	6.0	3
	478–750	3.924	10.938	4.142	3.9	4
Mo	422–550	0.493	3.560	...	12.6	5
	550–730	−3.814	...	...	2.6	6
Pd	440–750	2.840	4.665	0.632	2.9	7
Th	449–746	6.231	10.719	1.910	4.8	8

[a] $\text{Log } X = A - B \times 10^{3}T^{-1} + C \times 10^{6}T^{-2}$. X = atom fraction of solute.

Table III. Distribution of Standard Deviations in Solubility Measurements

Solute	Solubility Equation	s_{obsd}	s_a^a	s_s	Δt_τ^0
Zr	1	5.7	2.1	5.3	1.7
	2	4.3	2.1	3.8	3.7
Nb	3	6.0	3.2	5.1	2.4
	4	3.9	3.2	2.2	1.4
Mo	5	12.6	1.1	12.5	15.6
	6	2.6	1.1	2.4	...
Pd	7	2.9	2.1	2.0	2.0
Th	8	4.8	1.4	4.6	2.3

[a] % standard deviation of standard samples analyzed concurrently with analytical samples.

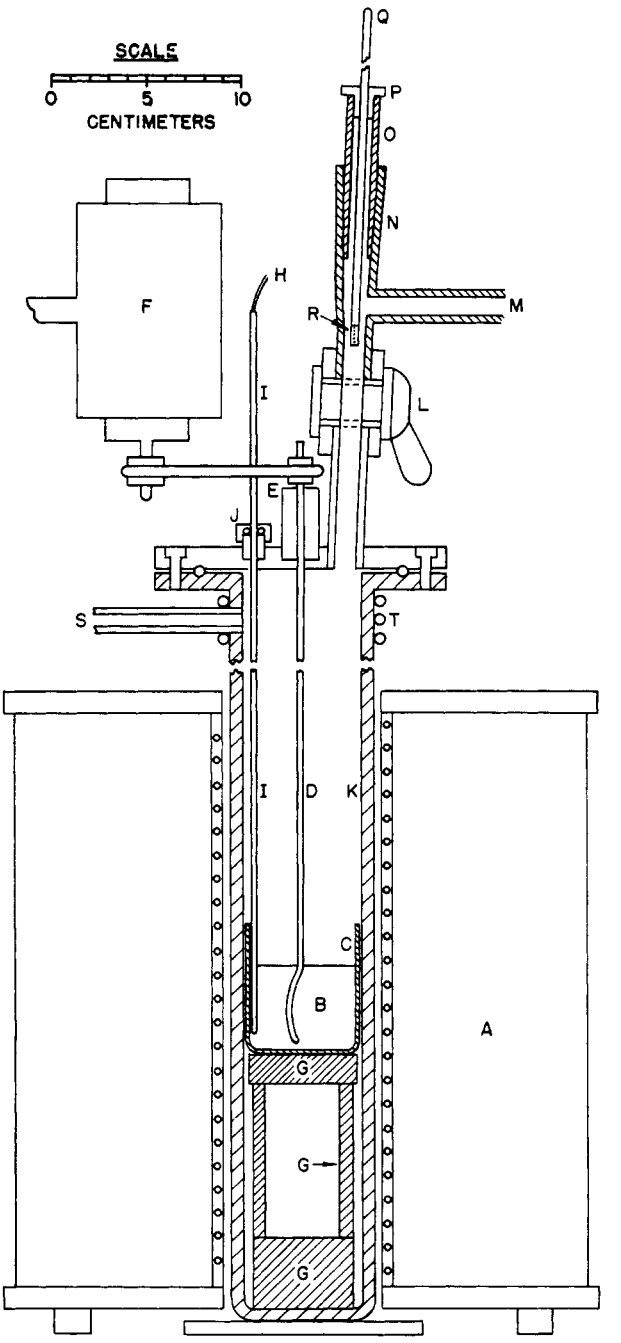

Figure 1. Solubility apparatus

A. Furnace (resistance type equipped with automatic temperature control)
B. Melt
C. Crucible (Morganite Triangle RR alumina or high purity graphite; see Table I)
D. Stirring rod (Ta, W, Nb or Mo; see Table I)
E. Stirrer bearing
F. Stirring motor
G. Refractory supports
H. Thermocouple (Chromel-Alumel)
I. Thermocouple protection tube (Morganite alumina or Vycor)
J. Vacuum coupling
K. Furnace tube (Type 310 stainless steel)
L. Stopcock (9-mm. bore)
M. To vacuum
N. Sampling lock (standard taper joint, female section)
O. Sampling lock (standard taper joint, male section)
P. Rubber serum cap
Q. Sampler (Vycor or Pyrex pipet)
R. Porous graphite filter (National Carbon Co., grade 60)
S. To vacuum ond helium
T. Cooling coil

the observed thermal-arrest temperature of a melt containing 0.6 weight % Zr was the same as that of pure zinc within the experimental accuracy of the measurement, ± 0.2° C. This observation indirectly confirms our solubility curve in the low temperature range.

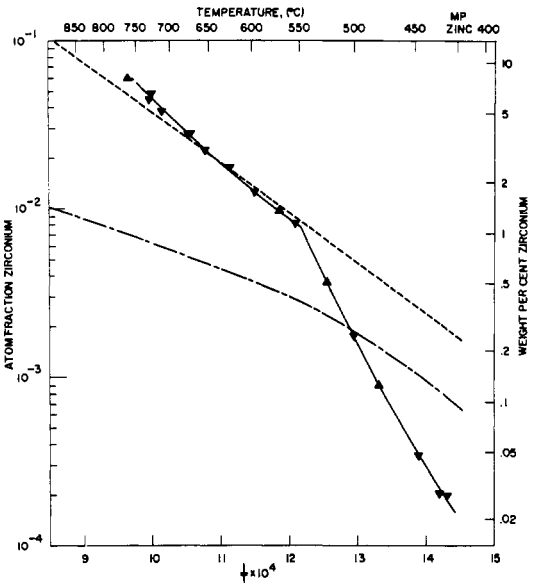

Figure 2. Solubility of zirconium in liquid zinc

—— Equations 1 and 2
▼ Falling temperature
▲ Rising temperature
····· Gebhardt (5)
– – – Chiotti and Kilp (2)

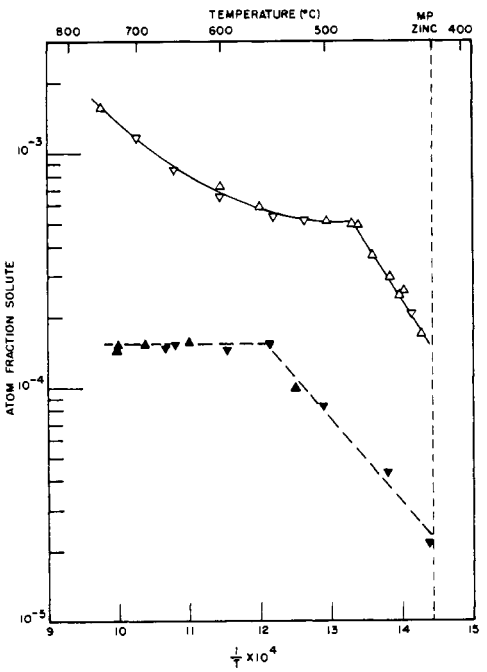

Figure 3. Solubility of niobium and molybdenum in liquid zinc

Niobium
—— Equations 3 and 4
▽ Falling temperature
△ Rising temperature
Molybdenum
– – – Equations 5 and 6
▼ Falling temperature
▲ Rising temperature

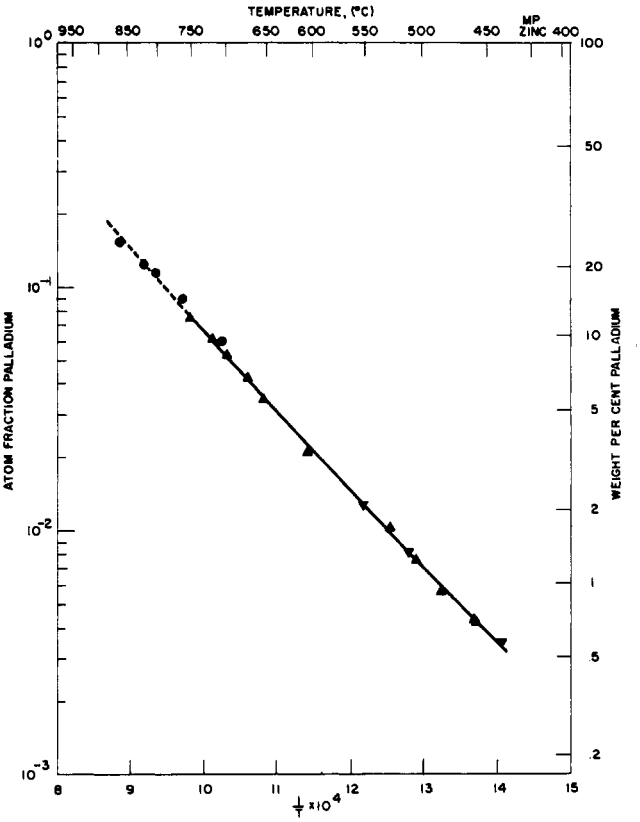

Figure 4. Solubility of palladium in liquid zinc

—— Equation 7
– – – Extrapolated
▼ Falling temperature
▲ Rising temperature
● Nowotny, Bauer, Stempfl (11) (thermal analysis)

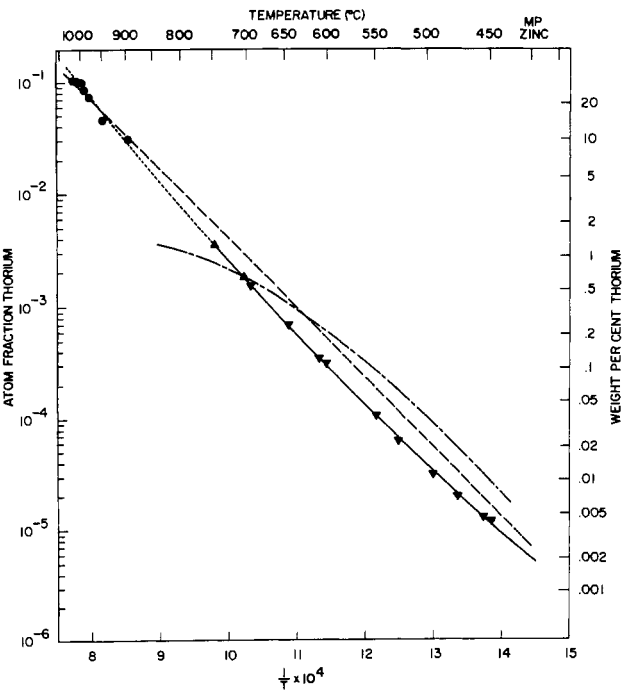

Figure 5. Solubility of thorium in liquid zinc

—— Equation 8
····· Extrapolated
▼ Falling temperature
▲ Rising temperature
····· Smirnov, others (12)
– – – Chiotti and Gill (1)
● Thermal analysis data

Because of the known stability of zirconium carbide, it was necessary to determine whether significant amounts of zirconium were removed from solution by the graphite filters during sampling. Accordingly, two unfiltered and three filtered samples were withdrawn consecutively at the same temperature. The average of the unfiltered samples, 0.031 weight %, was not significantly higher than that of the filtered samples, 0.028%.

The marked disagreement between our liquidus line and Gebhardt's (5) is not surprising because his method, thermal analysis, is not as precise as the solubility method for the establishment of liquidus lines when solute concentrations are small. Our liquidus line is in agreement with that of Chiotti and Kilp (2) above 545° C., where they made vapor pressure–composition measurements and solubility determinations without filtration. The agreement is poor below the peritectic, where their curve is based on only two measurements— a solubility determination at 500° C. and metallographic estimate of the eutectic composition. The latter is of questionable value in a system such as this, in which the volume of one phase in the eutectic structure is much smaller than that of the other.

Niobium. The solubility data, shown in Figure 3, are in rough agreement with data obtained above 600° C. at Iowa State College (8).

The intersection of the two segments of the solubility curve at 478° C. indicates a peritectic reaction. Its existence was confirmed by metallographic observations and by a thermal arrest at 485° C. obtained with a 10 weight % niobium-zinc alloy heated at about 0.5° per minute.

Crystals of the solid phase in equilibrium with the melt at temperatures above this peritectic were isolated from an ingot by selective dissolution of the zinc matrix with dilute hydrochloric acid. An x-ray study (4) of this phase revealed an ordered cubic structure of the $AuCu_3$ type ($L1_2$) with a_0 = 3.932 A., ρ_x = 7.893 grams per cc. The mean pycnometric density was 7.83 grams per cc. This phase was identified as $NbZn_3$ by chemical analysis of the isolated crystals and by a powder-metallurgy synthesis. The solid phase in equilibrium with the melt below the peritectic temperature has not been identified. The structure of $NbZn_3$ is the subject of a recent article by Vold (13)

Molybdenum. The solubility data are shown in Figure 3. The intersection of the two segments of the solubility curve at 550° C. indicates a peritectic reaction. Its existence was confirmed by thermal analysis. Metallographic observations revealed that the phase in equilibrium with the melt below the peritectic is an intermetallic phase, whereas at higher temperatures it is molybdenum.

Crystals of the intermetallic phase, formed by annealing below the peritectic and isolated by selective dissolution with dilute hydrochloric acid, contained 22.0% molybdenum, 72.8% zinc, and 0.001% iron. An x-ray study (4) revealed a face-centered cubic lattice, a_0 = 7.72 A. This phase, possibly $MoZn_6$, was also identified as the major component in a 14 atom % molybdenum powder compact annealed at 525° C.

Very little work on the Zn-Mo system has been reported. Guertler (6) observed some solubility of molybdenum in molten zinc and the formation of an unidentified intermetallic phase on cooling. Koster and Schmid (9) stated that pure molybdenum and zinc do not alloy at 1200° C. Both observations are consistent with our data.

Palladium. The solubility data are shown in Figure 4. Our curve, extrapolated to 890° C., is in good agreement with data obtained by Nowotny, Bauer, and Stempfl (11) by thermal analysis of melts containing at least 10 weight % palladium.

The zinc-palladium phase diagram (7) in the zinc-rich region is not well established, but the solid phase(s) has been reported to be of the gamma-brass type(s).

Thorium. The solubility data and those obtained by Smirnov and others (12) and Chiotti and Gill (1) are shown in Figure 5. The earlier determinations, obtained by analysis of unfiltered samples of settled melts, are generally higher than ours and show more scatter.

The most zinc-rich intermetallic phase in the zinc-thorium system is Th_2Zn_{17} (10), which melts congruently at 1015° C. Up to this temperature, the solubility curve should show no breaks. Our solubility curve was extrapolated to this melting point and found to agree well with the data obtained by Chiotti and Gill (1) by thermal analysis of melts containing more than 9.4% thorium.

Analysis of Deviations. The observed standard deviation, s_{obsd}, has been separated into s_a, that due to chemical analysis, and s_x, that due to all other sources such as differences between the true temperatures at the sampling points and the measured temperatures, the existence of under- or oversaturation, etc. The meaning of s_x is more readily understood when it is expressed as the equivalent temperature variability, Δt_x, at the mid-range temperature. Values of these quantities are given in Table III.

CONCLUSIONS

One of the methods for the measurement of solubilities in liquids is the chemical analysis of samples of the saturated liquid. It is particularly useful for measuring low solubilities in metals, when suitable precautions are taken to ensure the attainment of equilibrium and to avoid the inadvertent inclusion of particles of the solid phase in the liquid samples.

A peritectic temperature in several systems has been determined by measurement of the temperature of intersection of segments of liquidus lines. Being based entirely on systems in equilibrium, this method may sometimes be more reliable than other methods.

Thermodynamic functions derived from this work will be discussed in a forthcoming article.

ACKNOWLEDGMENT

The authors thank C.G. Wach, R.J. Uhle, and G.M. Kesser for valuable technical assistance. They also express appreciation to D.S. Flikkema and B.S. Tani for making their x-ray data available before publication, and to I. Johnson and T. F. Young for many valuable contributions.

LITERATURE CITED

(1) Chiotti, Premo, Gill, K.J., *Trans. Am. Inst. Mining Met. Engrs.* **221**, 573 (1961).
(2) Chiotti, Premo, Kilp, G.R., *Ibid.*, **215**, 892 (1959).
(3) Feder, H.M., Teitel, R.J., Proceedings of Second International Conference on Peaceful Uses of Atomic Energy, Vol. **17**, p. 383, Geneva, 1958.
(4) Flikkema, D.S., Tani, B.S., private communication.
(5) Gebhardt, Erich, *Z. Metallk.* **33**, 355 (1941).
(6) Guertler, W., *Ibid.*, **15**, 151 (1923).
(7) Hansen, Max, Anderko, Kurt, "Constitution of Binary Alloys," 2nd ed., McGraw-Hill, New York, 1958.
(8) Iowa State College Metallurgy Quarterly Rept. (I.S.C. 644) April–June 1955 (Feb. 9, 1956).
(9) Koster, Werner, Schmid, Heinz, *Z. Metallk.* **46**, 462 (1955).
(10) Makarov, E.S., Vinogradov, S.I., *Kristallografiya* **1**, 634 (1956).
(11) Nowotny, H., Bauer, E., Stempfl, A., *Monatsh. Chem.* **82**, 1086 (1951).
(12) Smirnov, M.V., Ilyushchenko, N.G., Detkov, S.P., Ivanovskii, L.E., *Zhur. Fiz. Khim.* **31**, 1013 (1957).
(13) Vold, C.L., *Acta Cryst.* **13**, 743 (1960).
(14) Youden, W.J., "Statical Methods for Chemists," Wiley, New York, 1951.

RECEIVED for review August 11, 1960. Accepted December 15, 1960. Presented in part before the Division of Industrial and Engineering Chemistry, 135th Meeting, ACS, Boston, Mass., April 1959. Research carried out under auspices of the U. S. Atomic Energy Commission.